Peter - This is fantastic! CHKW

MAE 427
FM 2

Wake Interference and Drag Reduction

Peter Polidoro
Fall 1998
Lab Section 10
Instructor: Raghuraman Govardhan

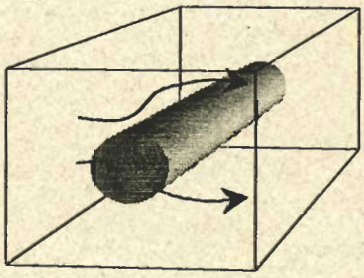

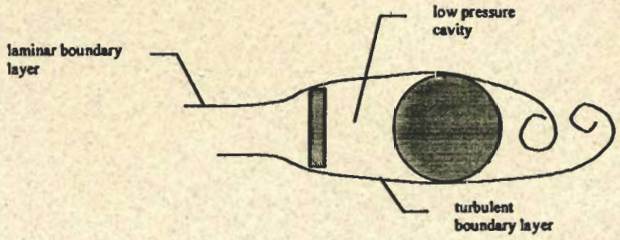

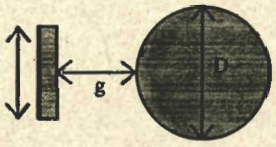

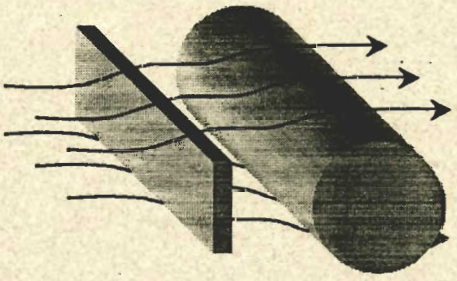

Table of Contents

✓

Great !

Abstract

The goals of this experiment were to examine the drag reduction on a cylinder in high Reynolds number flow caused by placing an interference plate in front of the cylinder, and to find the optimum geometry to minimize the plate/cylinder system drag. Previous experiments have been done on the drag reduction by objects behind the body in the flow, but only recently have experiments been done that place an interference object in front of the body. Using a wind tunnel, a horizontal cylinder with pressure ports drilled along the circumference, and various sized metal vertical plates, we found that we were able to drastically reduce the drag on the cylinder by placing the plates upstream from it. The cylinder drag was reduced because the interference plate tripped the boundary layer into turbulence, which reduces the wake behind the cylinder, increasing the pressure on the back of the cylinder and reducing the net pressure force on the cylinder in the downstream direction. In a mode of flow called cavity flow, the net pressure on the cylinder in the downstream direction, and therefore the cylinder drag, was further reduced because of a low-pressure cavity created between the front of the cylinder and the back of the plate. We found an optimal ratio of the diameter of the cylinder to the distance from plate front to cylinder back to be around 1.5. The optimal plate width to cylinder diameter ratio was around 40%, but very similar reductions in the drag could be had in the large ratio range of about 30% to 70%. When the dimensions of the plate/cylinder system were in their optimal configuration, the drag on the cylinder was so low that the drag of the plate and the cylinder combined was about 40% of the drag on a cylinder in the same flow without a plate. We illustrated the importance of these results by calculating that a truck using an interference plate might be able to travel almost 36% faster for the same power output.

Please note that it is good to state the value of Re.

Great summary!

Method

Apparatus

Wind Tunnel:

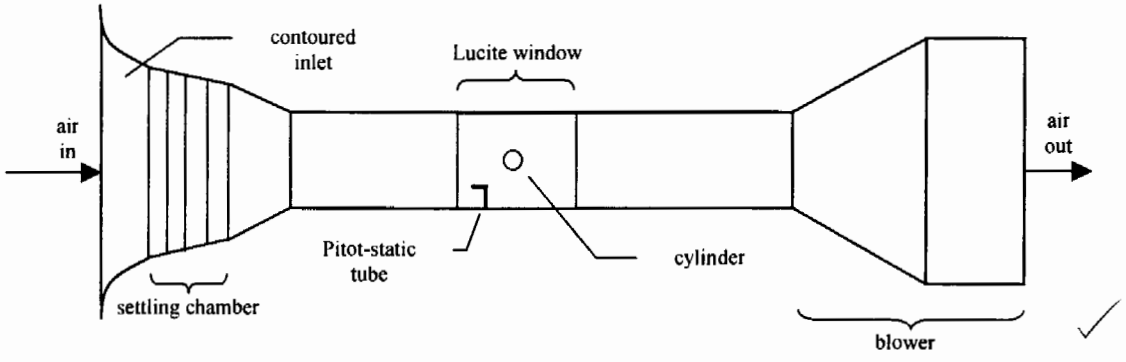

Figure 1 - Wind tunnel.

Great sketch!

The wind tunnel draws air down a long rectangular test section with a blower powered by a 25 hp motor. A contoured inlet reduces edge effects on the entering flow and a settling chamber containing screens and honeycombs largely reduces the turbulence level, improving the flow uniformity into the test section. The flow enters a constriction section after leaving the settling chamber, which increases the flow speed. The flow enters the settling chamber before it is accelerated to reduce the power requirements on the blower motor. The horizontal cylinder is located midway down the test section, surrounded by a clear Lucite window. A Pitot-static tube is placed in the flow to measure the flow speed.

Pitot-Static Tube:

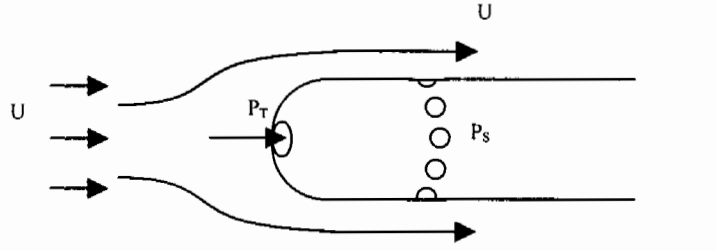

Figure 2 - Pitot-static tube.

Flow speed can be calculated from pressure measurements made with a Pitot-static tube. The Pitot-static tube measures the pressure of the air moving at the free-stream velocity (P_S) and measures the pressure of the air after it is decelerated to zero velocity (P_T). Using Bernoulli's equation:

Bernoulli's equation, assuming constant fluid density:

$$P_1 + \tfrac{1}{2}\rho U_1^2 = P_2 + \tfrac{1}{2}\rho U_2^2$$

P_1, P_2 = two fluid pressures
ρ = fluid density
U_1, U_2 = two fluid flow rates at corresponding fluid pressures

the fluid velocity can be solved for in terms of the measured pressure difference. In our case, $P_1 = P_T$, $U_1 = 0$, $P_2 = P_S$, $U_2 = U$, so:

Bernoulli's equation for our the Pitot-static tube:

$$U = [2(P_T - P_S)/\rho]^{1/2}$$

The transducer we used to measure the pressure difference gives the measurement in units of mm Hg. These units can be converted to dimensions of pressure by multiplying by the density of mercury and the gravitational constant. Rearranging Bernoulli's equation further and determining an appropriate conversion factor that will yield the fluid speed in units of meters per second:

Equation for fluid speed (m/s) as a function of the pressure transducer reading:

$$U = 15.20[\Delta h]^{1/2}$$

Δh = pressure transducer reading in mm Hg

1

The ultimate goal of the determining the flow speed is to calculate the Reynolds number of the air flowing past the cylinder.

Definition of the Reynolds number:

$$Re = Ud/\mu$$

d = cylinder diameter
μ = dynamic viscosity coefficient

2

FANTASTIC WORK!

Bare Cylinder Measurements

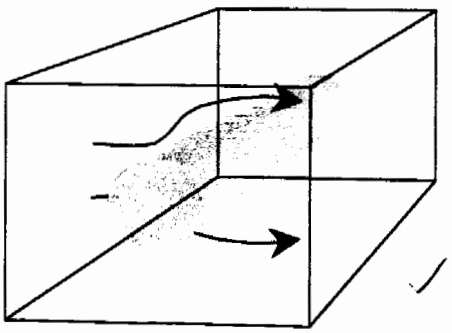

Nice figure!

The cylinder can be a bit darker.

Figure 3 - Air flowing past the horizontal cylinder in the Lucite window.

The goal of this section is to measure the coefficient of drag on a horizontal cylinder in high Reynolds number air flow. The drag coefficient is a non-dimensionalized measure of the drag force on the obstacle in the flow.

Definition of the drag coefficient:

$$C_D = D[\tfrac{1}{2}\rho U^2 dL]^{-1}$$

C_D = coefficient of drag
D = drag force on the body
L = body length

The drag force on the body in the flow arises from normal stresses due to the pressure at the surface of the body and from the tangential stresses due to the viscous friction forces. There are several ways to measure the drag force on a body. The body can be mounted on springs and a force balance can be done knowing the displacement of the springs. A second approach is to do a momentum balance on a control volume around the cylinder. A third method is to measure the pressure distribution around the circumference of the body. In this last method, the friction force on the body is ignored. This is reasonable, since the viscous friction force on the body is inversely proportional to the square root of the Reynolds number and becomes negligible at high Reynolds numbers (approximately 1% of the total drag force.) In our experiment, we chose to measure the drag force on the cylinder by measuring the pressure distribution around the circumference of the cylinder. The measurements are relatively easy to make, are accurate, and will provide insight to the flow patterns around the cylinder.

Good point!

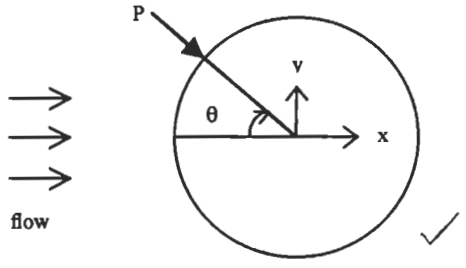

Figure 4 - Pressure distribution around the circumference of the cylinder.

Drag force on a body as a function of the pressure around the circumference:

$$D = \oint P dy = 2\int_{0\ \text{front}}^{d/2} P dy - 2\int_{0\ \text{rear}}^{d/2} P dy$$

The surface pressure can be normalized to a non-dimensional pressure coefficient:

Definition of the pressure coefficient:

$$C_P = [P - P_S][\tfrac{1}{2}\rho U^2]^{-1} = [P - P_S][P_T - P_S]^{-1}$$

Substituting the definition of the pressure coefficient into the formula for the drag force yields an equation for the coefficient of drag:

Coefficient of drag as a function of the pressure coefficient:

$$C_D = 2\int_{0\ \text{front}}^{d/2} C_P dy - 2\int_{0\ \text{rear}}^{d/2} C_P dy$$

We measured the pressure at the discrete intervals around the circumference of the cylinder.

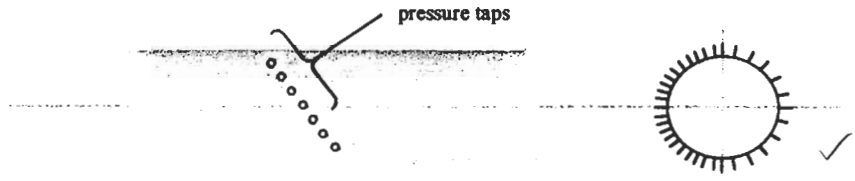

Figure 5 - Location of the pressure taps around the circumference of the cylinder.

The pressure taps were located at various intervals along the surface of the cylinder from 0 to 360°. There were 34 holes in total, each with a diameter of 0.018", and they were slightly staggered to minimize any interference effects between holes. Each hole from 0 to 180° was connected to its corresponding hole in the range of 180 to 360° with a single tube that averaged the pressure readings of the two holes, so that 18 readings were required to obtain the pressure variation around the cylinder. Since the measurements were taken at discrete intervals, the integrals in the equation for the coefficient of drag need to be replaced with summations. The 18 pressure coefficients can be added together to give the drag coefficient, but they must first be scaled by weighting factors that determine how much each pressure coefficient at a particular angle contributes to the pressure drag force. For example, the pressure at the very top of the cylinder (90°) does not contribute at all to the pressure drag in the horizontal direction, so the weighting factor for the 90 ° hole is zero. The weighting factor is a function of the sine of the angles slightly above and below each hole. The values for the weighting function for each hole can be found in Appendix A.

The equation for the drag coefficient in discrete form:

$$C_D = \Sigma C_{Pn} W_n$$

C_{Pn} = pressure coefficient at hole n

W_n = weighting function at hole n

4

To measure the pressure coefficient at each of the 18 locations, the 18 tubes connecting the 34 holes, along with the two tubes from the Pitot-static tube, were all connected to a scani-valve. The scani-valve is a large switch that allows two of the pressure readings to be sent to a very accurate capacitance pressure transducer, which measures the difference between the pressures and outputs the reading as a voltage. The voltage is later averaged (the pressures fluctuate in turbulent flow conditions) and is converted to the units of mm Hg. Every pressure reading along the circumference of the cylinder is compared to P_S from the Pitot-static tube and then converted to a pressure coefficient using equation 3. The drag coefficient for the cylinder can then be found using equation 4 and computed values of the weighting function.

Interference Plate Measurements

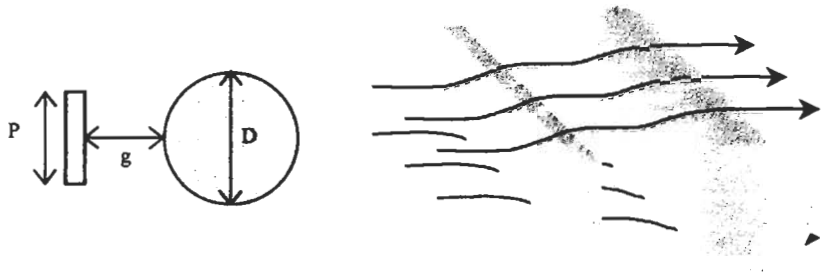

Figure 6 - Interference plate setup.

Great sketch!

The goals of this section are 1) to examine how a vertical plate placed in front of the cylinder can reduce the drag coefficient of the cylinder and the plate/cylinder system, and 2) to find the dimensions that minimize the system drag. We know from previous experiments that tiny plates placed in front of a cylinder can significantly reduce the system drag. Since small plates offer an improvement over no plate and very large plates would be worse than the bare cylinder alone, we suspect that there is an optimal P/D ratio that provides the minimum amount of system drag. We measured the drag coefficient for the cylinder with two plate sizes (P/D = 11% and 34%) at a variety of locations in front of the cylinder (g/D = 0.5, 1.5, 3.0, and 5.0.) We measured the drag coefficient in the same way that we measured it for the bare cylinder, except we used a computer to automatically switch the scani-valve positions, record the data, and compute the corresponding drag coefficient. This sped up the process and allowed us to examine several cases in a relatively short amount of time. To calculate the coefficient of drag for the plate/cylinder system, we need to estimate the drag force on the plate. The total drag of the system is equal to the drag on the cylinder added to the drag on the plate.

Equation for the system drag:

$$D_{sys} = D_{cyl} + D_{plate} = C_{Dc}(0.5\rho U^2 D) + C_{Dp}(0.5\rho U^2 P)$$

D_{sys} = total system drag
D_{cyl} = cylinder drag
D_{plate} = plate drag
C_{Dc} = cylinder drag coefficient
C_{Dp} = plate drag coefficient

Previous experiments indicate that a conservative estimate of the plate drag coefficient is 1.4. Using this estimate, we can rearrange the above equation to give:

Equation for the system drag coefficient to cylinder drag coefficient ratio:

$$C_{Dsys}/C_{Dbare} = (C_{Dc}/C_{Dbare}) + (1.4/C_{Dbare})(P/D)$$

C_{Dbare} = drag coefficient of the bare cylinder (no interfering plate)

Results and Discussion

Drag Coefficient and Pressure Distribution for Bare Cylinder

Re = 46,300	$C_D = 1.21$

The pressure distribution for the bare cylinder can be found on the plot "Bare Cylinder vs. Potential Flow Pressure Distribution" in Appendix B. Also shown on the graph is the pressure distribution for the idealized potential flow scenario. The exact solution for frictionless incompressible potential flow is obtained by superposing a uniform stream and a doublet. In potential flow, the streamlines of the flow are found to be symmetric about a vertical axis through the center of the cylinder.

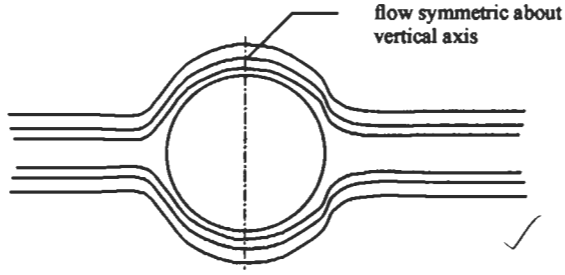

Figure 7 - Potential flow around a cylinder.

Good idea to sketch this!

Using Bernoulli's equation, we find that $C_P = (1 - 4\sin^2\theta)$ for potential flow. Since C_P is symmetric about the vertical axis, the coefficient of drag on the cylinder is zero. The pressure distribution we measured for the bare cylinder differs substantially from the idealized potential flow, however. The distributions look fairly similar until theta reaches approximately 40 degrees, then the pressure tends to level off for the bare cylinder, while dipping down and back up for the potential flow. The cause for the discrepancy is boundary layer separation that occurs on the bare cylinder. Boundary layer separation is a characteristic of real flow around bluff bodies and is due to fluid particles being subjected to adverse pressure gradients. As the fluid particles in the free stream encounter the front surface of the cylinder, they pick up speed and the local region of air decreases in pressure. The boundary layer is laminar as long as the pressure in front of the particle is lower than the pressure behind the particle. As the velocity of the particles begin to decrease, however, as they flow around the body, the pressure increases and the particles encounter an adverse pressure gradient and are flowing from regions of lower pressure into higher pressure. The boundary layer can no longer remain laminar and it separates and rolls into a spiral of turbulent vorticity, which sheds from each side of the cylinder in alternating antisymmetric patterns. The vorticies must be shed in an antisymmetric pattern to maintain stability.

It is better to say 'attached'.

} 'attached'

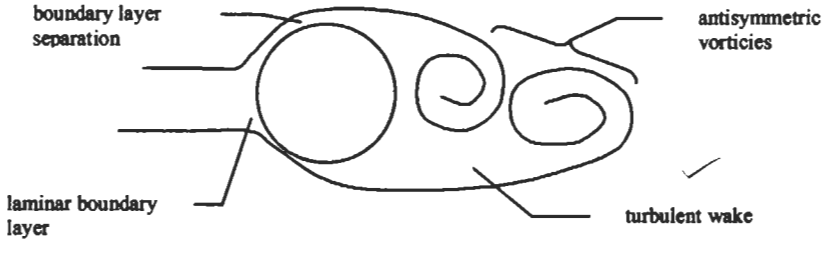

Good sketch!

Figure 8 - Real flow around a bluff body.

A vortex must have an inward pressure gradient to provide the centripetal force necessary to maintain its shape. These low-pressure vorticies at the rear of the cylinder lower the pressure at the back surface and cause a net pressure force on the cylinder in the direction of the free stream flow. This approximately constant negative pressure distribution on the back face of the cylinder can be seen on the pressure distribution graph in the 90 to 180 degree range. The negative pressure on the back face is responsible for the large drag force on blunt objects in real flow. The pressure distribution that we measured is very similar to the pressure distribution measured by Fage and Falkner (1931) for laminar flow over a cylinder. The main similarity is the nearly constant pressure region from 90 to 180 degrees across the back face of the cylinder. The pressure coefficient at the very rear of the cylinder (C_{Pb}) was measured to be –1.28 (see Table 1 in Appendix B). This is almost identical to the C_{Pb} found by Williamson (1993.) These similarities are an indication that the flow around the bare cylinder started as laminar and then separated into a turbulent wake that caused the high discrepancy between our measured pressure distribution and that of the idealistic potential flow.

The angle at which the boundary layer separates from the cylinder can be estimated from the pressure distribution curve. An inflection point on the pressure distribution curve generally marks the position of flow separation. The inflection point must occur in a region of increasing slope, since this is the adverse pressure gradient region. The separation seemed to occur at approximately 75° (see Table 1 in Appendix B.) This very nearly agrees with Hiemenz (1911), who found the boundary layer separation angle to be 82° on a circular cylinder. This is another indication that the flow in the boundary layer up to the point of separation is steady and not turbulent.

Very Good!

Mechanisms for Drag Reduction

Introducing a plate in front of the cylinder drastically changed the pressure distribution around the cylinder surface. This can be seen on the graph "Cylinder Pressure Distributions – P/D = 34%", found in Appendix B. The first thing to notice is that while the pressure on the back face of the cylinder is still negative with the interference plates in front of the cylinder, it is much higher than the pressure at the back face of the bare cylinder. Increasing the pressure on the back pressure goes a long way in reducing the drag on the cylinder, since most of the drag is due to the "suction" caused by the negative pressure region. Another thing to notice on this graph is that the pressure at the very front of the cylinder was decreased in both the g/D = 1.5 case and the g/D = 5.0 case. Lowering the front pressure has the same affect as raising the rear pressure, namely the net "suction" force is decreased and the cylinder drag is reduced. The pressure coefficient at the back face of the cylinder (g/D = 1.5 case) is –0.56 and the angle of separation is approximately 105°. These results are nearly identical to the back face pressure and the angle of separation found by Fage and Falkner (1931) for turbulent flow (see Table 1 in Appendix B.) This suggests that the boundary layer that reaches the cylinder is already turbulent. This turbulent boundary layer separates further rearward than if it were laminar and causes thinner and weaker vorticies to form, which narrows the wake and increases the pressure on the back face of the cylinder.

Very Good!

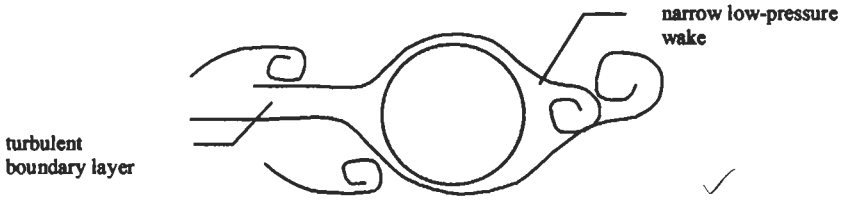

Figure 9 - Turbulent boundary layer on the front cylinder surface.

Both the case of g/D = 1.5 and the case of g/D = 5.0 reduced the cylinder drag coefficient significantly. C_D was lowered to .47 from 1.21 when P/D = 34% and g/D = 5.0 and in the case of P/D = 34% and g/D = 1.5, the drag coefficient for the cylinder was reduced to an amazingly low 0.068. The cylinder drag for the g/D = 1.5 case was nearly zero and the nearly symmetric and constant pressure distribution curve indicates why. A major contributing factor to the super-low drag coefficient is the negative pressure at the very front of the cylinder. This causes a "suction" force on the front face that opposes the "suction" force on the back face that was responsible for the large drag on the cylinder. The pressure on the front face of the cylinder in the g/D = 5.0 case is positive, however. The reason one is positive and the other is negative is due to two distinct flow types occurring in these two cases. In the case of g/D = 5.0, the mode of flow is referred to as wake impingement flow. The plate creates a turbulent boundary layer that encounters the front surface of the cylinder.

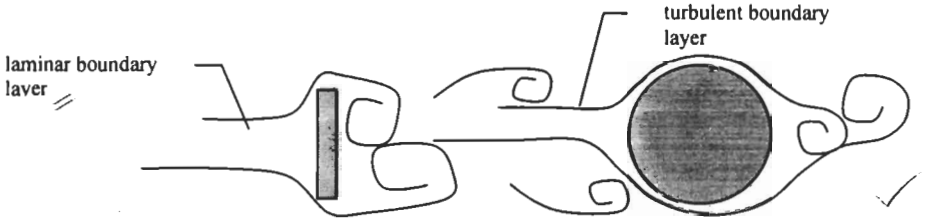

Please note that the boundary layer starts only at the plate.

Figure 10 - Wake impingement flow mode.

The other mode of flow is referred to as cavity flow. In this case, the plate still trips the boundary layer into turbulence, but the plate is close enough to the cylinder that the flow cannot form vorticies behind the plate, rather the boundary layer reattaches itself to the sides of the cylinder. The region in between the back of the plate and the front of the cylinder is at low pressure and helps reduce drag on the cylinder.

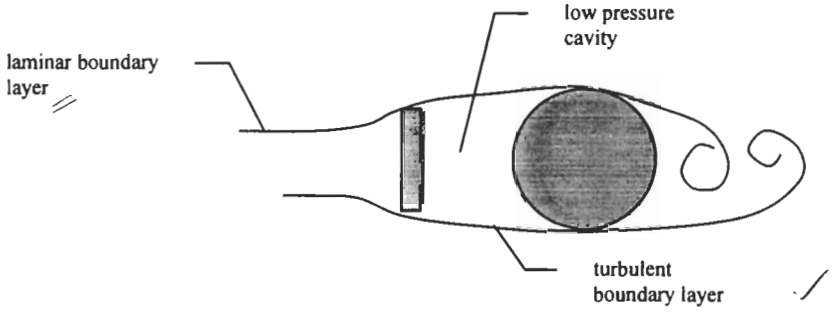

free shear layer

turbulent boundary layer on the cylinder

Please note the definition above.

Figure 11 - Cavity flow mode.

At most g/D ratios, the flow is either cavity flow mode or wake impingement mode. At certain g/D ratios, however, the flow cannot "decide" which mode to be in, so it oscillates back and forth between the two. This is referred to as bi-stable flow, since there are two stability regions that the flow can "jump" back and forth between.

Optimum Drag Reduction

As argued in the methods section, we assume that there exists an optimal P/D ratio that minimizes the drag on the plate/cylinder system. As we saw earlier, the g/D ratio can also affect drag on the system.

The drag on the cylinder is reduced when the flow is in cavity mode rather than the wake impingement mode. The "Interference Plates and the g/D Ratio" graph in Appendix B shows how the system drag to cylinder drag ratio is affected by various g/D ratios. In both the P/D = 11% and the P/D = 34% cases, the drag ratio is at a minimum in a range of g/D = 1.5 to g/D = 2.5 for the cavity flow mode. Any of these values would theoretically be good for minimum system drag, but at g/D ratios of greater than about 2, we have to start worrying about entering the bi-stable flow mode. Therefore, we can pick a g/D ratio of 1.5 as a good ratio to try to minimize the P/D ratio about. The graph of "Minimum Cylinder Drag" in Appendix B shows how the cylinder drag varies as a function of the P/D ratio. The case of zero drag occurs somewhere around P/D slightly less than 0.4. The graph of "Minimum System Drag" in Appendix B shows how the drag on the plate/cylinder system varies as a function of P/D. (The equations for the drag calculations can be found in the methods section.) This graph shows very encouraging results. It seems that the drag of the entire plate/cylinder system can be reduced to almost 40% of the drag on the bare cylinder alone. The curve is also very flat, which means that the drag is very close to minimum at a large range of P/D ratios and is therefore fairly insensitive to the which P/D ratio is chosen. The P/D ratio range of 0.3 to 0.75 seems to produce minimum system drag. Our results support this conclusion since the P/D ratio of 0.34 that we tested had a much lower value of system drag than the P/D ratio of 0.11.

Good!

Excellent Work! Fantastic Presentation and great use of figures!

Good clear writing too!

97%

Keep it up

Conclusion

We found that we were able to drastically reduce the drag on a cylinder by placing a vertical plate upstream from it. The cylinder drag was reduced because the plate tripped the boundary layer into turbulence, which reduces the wake behind the cylinder, increasing the pressure on the back of the cylinder and reducing the net pressure force on the cylinder in the downstream direction. In the cavity flow mode, the net pressure on the cylinder in the downstream direction, and therefore the cylinder drag, was further reduced because of the low-pressure cavity created in the front of the cylinder. We found an optimal ratio of the diameter of the cylinder to the distance from plate front to cylinder back to be around 1.5. The optimal plate width to cylinder diameter ratio was a large range from about 30% to 70%. When the dimensions of the plate/cylinder system were in their optimal configuration, the drag on the cylinder was so low that the drag of the plate and the cylinder combined was about 40% of the drag of a cylinder in the same flow without a plate.

Very Good!

These findings could prove to be very useful for reducing drag on practical engineering applications. Anytime that fluid flows around a cylinder in a constant direction with a high Reynolds number, the system drag can be reduced by placing a plate of appropriate size in front of it. An obvious idea is to try to place plates in front of fast moving vehicles to reduce power loss to aerodynamic drag. Other places where this technology may be useful are where cylinders are subjected the forces from water current. Assuming that the Reynolds number is high enough for the phenomenon to take place, the drag on bridge pilings, dam gates, and possibly on the waders of a fisherman standing in a fast-moving stream could be reduced by rigging flat plates in the appropriate places.

Good ideas

Postscript

The significance of drag reduction can be illustrated by considering a truck with an interference plate placed on the front.

Power balance on bare truck vs. interference plate cases, assuming constant power output:

$$D_{sys}U_{sys} = D_{bare}U_{bare}$$

D_{sys} = drag on truck with interference plate
D_{bare} = drag on truck without interference plate
U_{sys} = velocity of truck with interference plate
U_{bare} = velocity of truck without interference plate

Substituting in the definition for the drag coefficients and solving for U_{sys}:

Velocity of truck with interference plate:

$$U_{sys} = U_{bare}[C_{Dbare}/C_{Dsys}]^{1/3}$$

C_{Dbare} = drag coefficient without interference plate
C_{Dsys} = drag coefficient with interference plate

Assuming the optimal drag ratio of 0.4 and U_{bare} of 100 mph, $\boxed{U_{sys} = 136 \text{ mph}}$

The 36% increase in velocity, while perhaps larger than could ever be obtained, would offer an enormous fuel savings.

Great Work!

Pressure Tap	theta	P-Ps (V)	Cp	Wn	Cp*Wn
1	home	---	---	---	---
2	Pt-Ps	0.6796	---	---	---
3	0	0.6803	1.00103	0.0872	0.0872
4	10	0.6114	0.899647	0.1717	0.15446
5	20	0.4087	0.601383	0.1638	0.09850
6	30	0.1032	0.151854	0.151	0.0229
7	40	-0.2609	-0.3839	0.1335	-0.0512
8	50	-0.6053	-0.89067	0.112	-0.0997
9	60	-0.8649	-1.27266	0.0872	-0.1109
10	70	-0.936	-1.37728	0.0474	-0.0652
11	75	-0.8886	-1.30753	0.0226	-0.0295
12	empty	---	---	---	---
13	empty	---	---	---	---
14	80	-0.8171	-1.20232	0.0151	-0.0181
15	85	-0.7813	-1.14965	0.0076	-0.0087
16	90	-0.7785	-1.14553	0	0
17	95	-0.7697	-1.13258	-0.0076	0.00860
18	100	-0.7758	-1.14155	-0.0518	0.05913
19	120	-0.7872	-1.15833	-0.1736	0.20108
20	140	-0.824	-1.21248	-0.266	0.32251
21	160	-0.8736	-1.28546	-0.3264	0.41957
22	180	-0.8687	-1.27825	-0.1736	0.22190
23	empty	---	---	---	---
24	empty	---	---	---	---
				Cd =	1.21231

P/D =	11%		
run	g/D	Cd	Cd/Cd bare
	0	1.212	1.000
1	0.5	0.9701	0.800
2	1.5	0.5896	0.486 (Optimum
3	3	0.66	0.544
4	5	0.7816	0.645

P/D =	34%		
run	g/D	Cd	Cd/Cd bare
	0	1.212	1.000
1	0.5	0.1223	0.101
2	1.5	0.0682	0.056 (Optimum
3	3	0.4103	0.338
4	5	0.4681	0.386

P/D =	34%	g/D =	0.5	Pt-Ps =
theta	P-Ps (V)	Cp	Cp*Wn	6.965
0	-3.635	-0.522	-0.0455	
10	-4.154	-0.596	-0.1024	
20	-4.236	-0.608	-0.0996	
30	-3.953	-0.568	-0.0857	
40	-2.534	-0.364	-0.0486	
50	-1.754	-0.252	-0.0282	
60	-4.065	-0.584	-0.0509	
70	-7.493	-1.076	-0.0510	
75	-8.761	-1.258	-0.0284	
80	-9.431	-1.354	-0.0204	
85	-9.603	-1.379	-0.0105	
90	-8.981	-1.289	0.0000	
95	-8.252	-1.185	0.0090	
100	-7.404	-1.063	0.0551	
120	-4.833	-0.694	0.1205	
140	-4.659	-0.669	0.1779	
160	-4.709	-0.676	0.2207	
180	-4.429	-0.636	0.1104	

P/D =	34%	g/D =	1.5	Pt-Ps =
theta	P-Ps (V)	Cp	Cp*Wn	6.9725
0	-3.722	-0.534	-0.0465	
10	-3.962	-0.568	-0.0976	
20	-3.881	-0.557	-0.0912	
30	-3.586	-0.514	-0.0777	
40	-2.966	-0.425	-0.0568	
50	-2.56	-0.367	-0.0411	
60	-3.216	-0.461	-0.0402	
70	-4.605	-0.660	-0.0313	
75	-5.452	-0.782	-0.0177	
80	-5.94	-0.852	-0.0129	
85	-6.487	-0.930	-0.0071	
90	-6.738	-0.966	0.0000	
95	-6.496	-0.932	0.0071	
100	-6.028	-0.865	0.0448	
120	-4.305	-0.617	0.1072	
140	-3.917	-0.562	0.1494	
160	-3.912	-0.561	0.1831	
180	-3.878	-0.556	0.0966	

P/D =	34%	g/D =	3	Pt-Ps =
theta	P-Ps (V)	Cp	Cp*Wn	6.8559
0	0.912	0.133	0.0116	
10	0.866	0.126	0.0217	
20	0.387	0.056	0.0092	
30	-0.66	-0.096	-0.0145	
40	-2.019	-0.294	-0.0393	
50	-3.978	-0.580	-0.0650	
60	-6.177	-0.901	-0.0786	
70	-7.999	-1.167	-0.0553	
75	-8.625	-1.258	-0.0284	
80	-8.644	-1.261	-0.0190	
85	-8.699	-1.269	-0.0096	
90	-8.572	-1.250	0.0000	
95	-7.861	-1.147	0.0087	
100	-7.551	-1.101	0.0571	
120	-5.237	-0.764	0.1326	
140	-4.525	-0.660	0.1756	
160	-4.266	-0.622	0.2031	
180	-3.971	-0.579	0.1006	

P/D =	34%	g/D =	5	Pt-Ps =
theta	P-Ps (V)	Cp	Cp*Wn	7.092
0	2.771	0.391	0.0341	
10	2.139	0.302	0.0518	
20	1.292	0.182	0.0298	
30	-0.187	-0.026	-0.0040	
40	-2.389	-0.337	-0.0450	
50	-4.862	-0.686	-0.0768	
60	-7.34	-1.035	-0.0902	
70	-9.129	-1.287	-0.0610	
75	-9.735	-1.373	-0.0310	
80	-9.664	-1.363	-0.0206	
85	-9.579	-1.351	-0.0103	
90	-9.194	-1.296	0.0000	
95	-8.935	-1.260	0.0096	
100	-8.36	-1.179	0.0611	
120	-5.653	-0.797	0.1384	
140	-4.638	-0.654	0.1740	
160	-4.522	-0.638	0.2081	
180	-4.093	-0.577	0.1002	

Appendix B

Optimization of Drag Reduction

U =	12.5	m/s
D =	5.54	cm
ν =	0.15	cm^2/s
Re =	46.3E+03	

Table 1

case	C_{Pf}	C_{Pb}	θsep	C_D
bare	1.00	-1.28	75	1.212
g/d = 1.5	-0.53	-0.56	105	0.068
turb. sep.	1	-0.6	105	0.520

P/D	Cd/Cd_bare	Cd_sys/Cd_bare
0	1.000	1.000
0.11	0.486	0.613
0.34	0.056	0.449
0.69	-0.350	0.447
1	-0.400	0.755

Good!

Bare Cylinder vs. Potential Flow Pressure Distribution

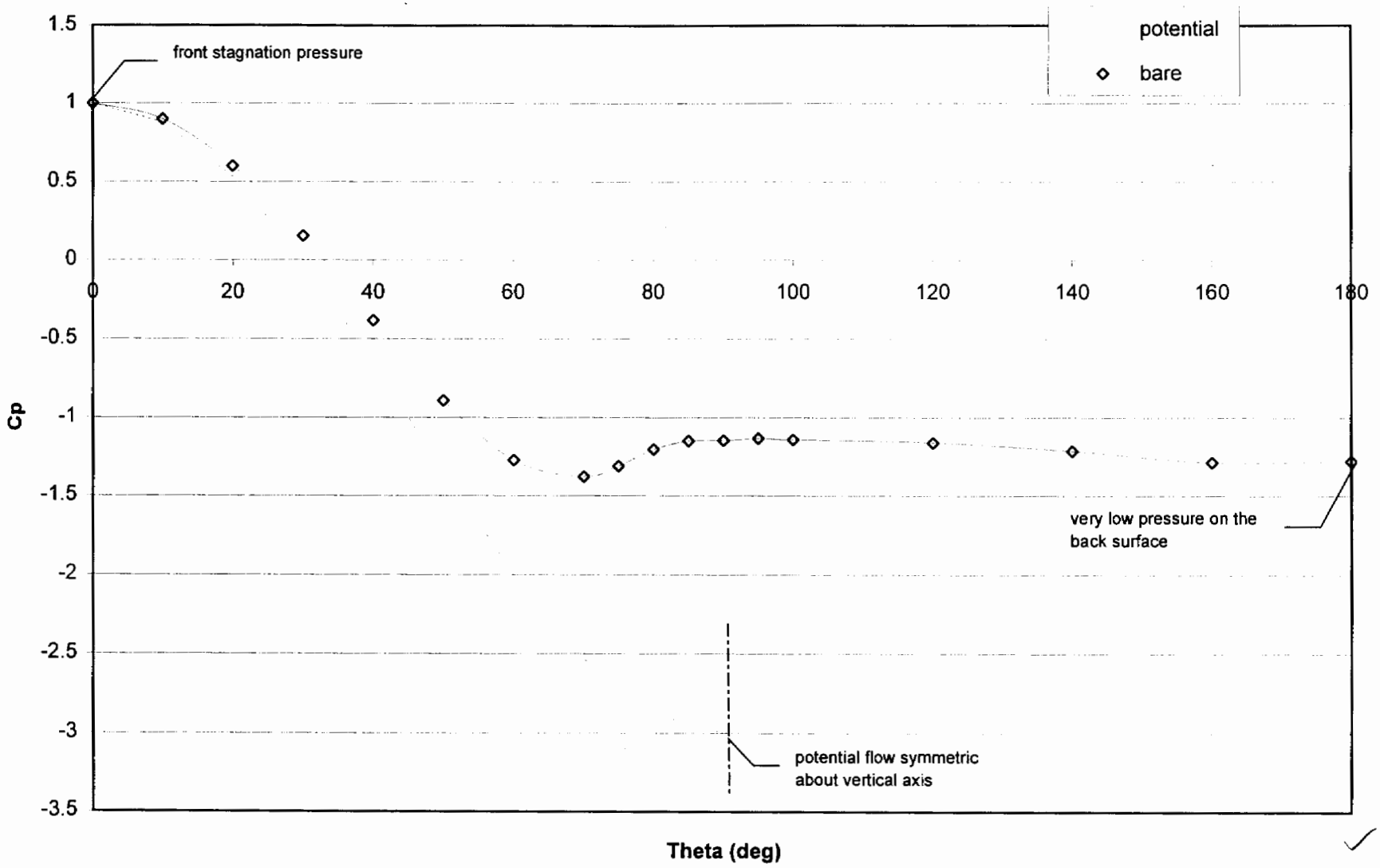

oops! The lines are very light

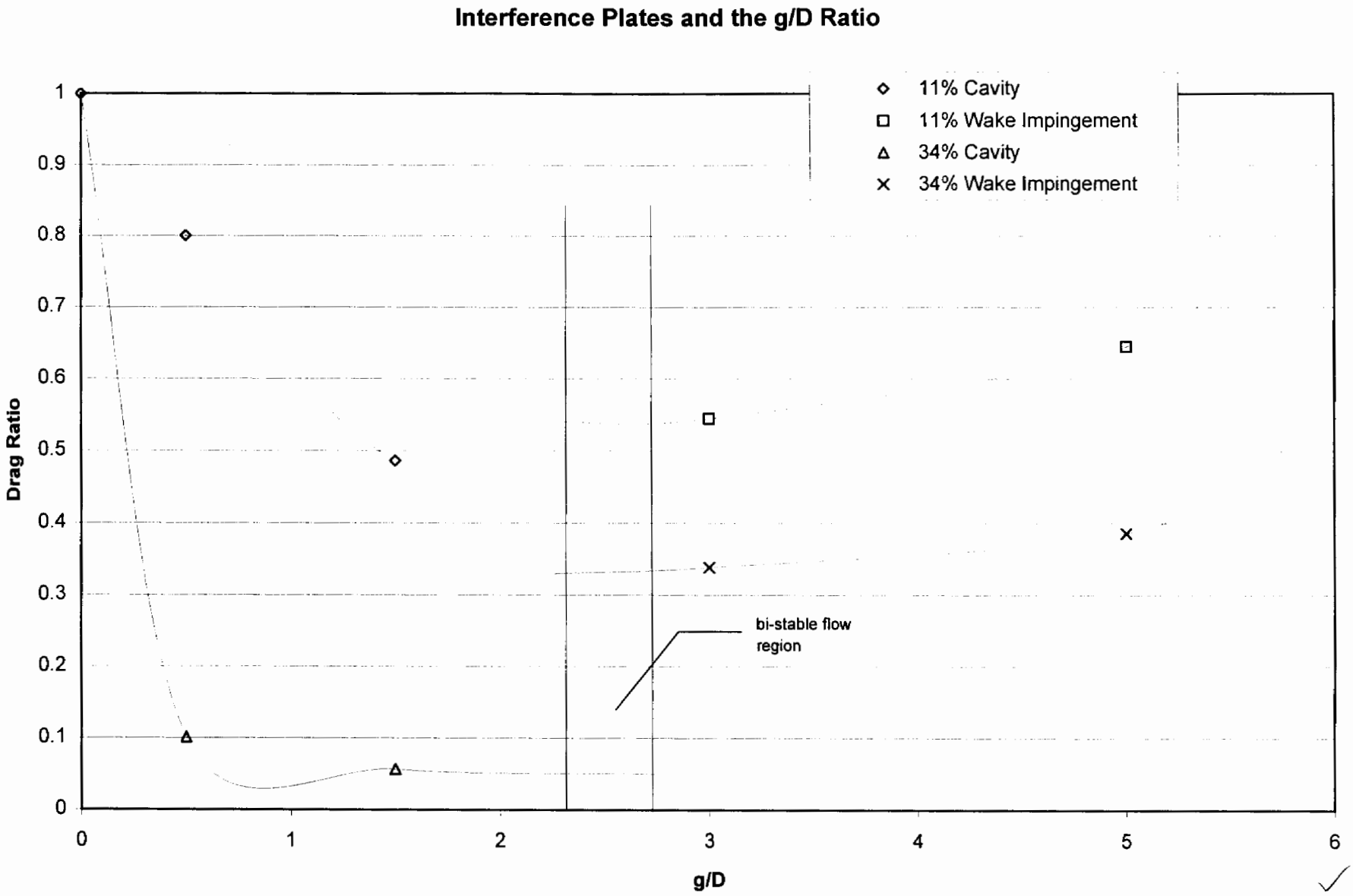
Interference Plates and the g/D Ratio
11% Cavity
11% Wake Impingement
34% Cavity
34% Wake Impingement
bi-stable flow region
Drag Ratio
g/D
0
0.1
0.2
0.3
0.4
0.5
0.6
0.7
0.8
0.9
1
0
1
2
3
4
5
6

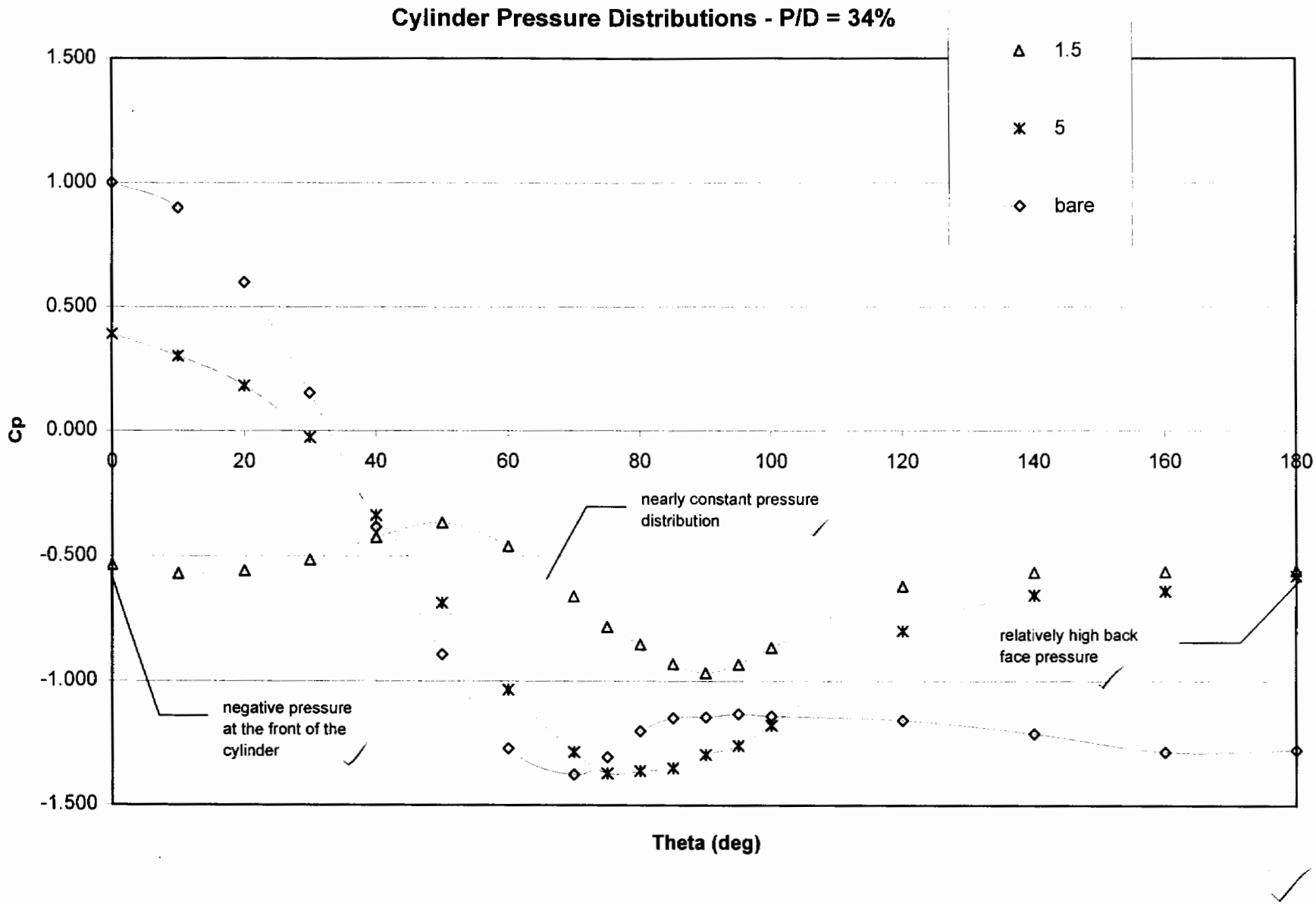
Cylinder Pressure Distributions - P/D = 34%
1.5
5
bare
1.500
1.000
0.500
0.000
-0.500
-1.000
-1.500
Cp
0
20
40
60
80
100
120
140
160
180
Theta (deg)
nearly constant pressure distribution
negative pressure at the front of the cylinder
relatively high back face pressure

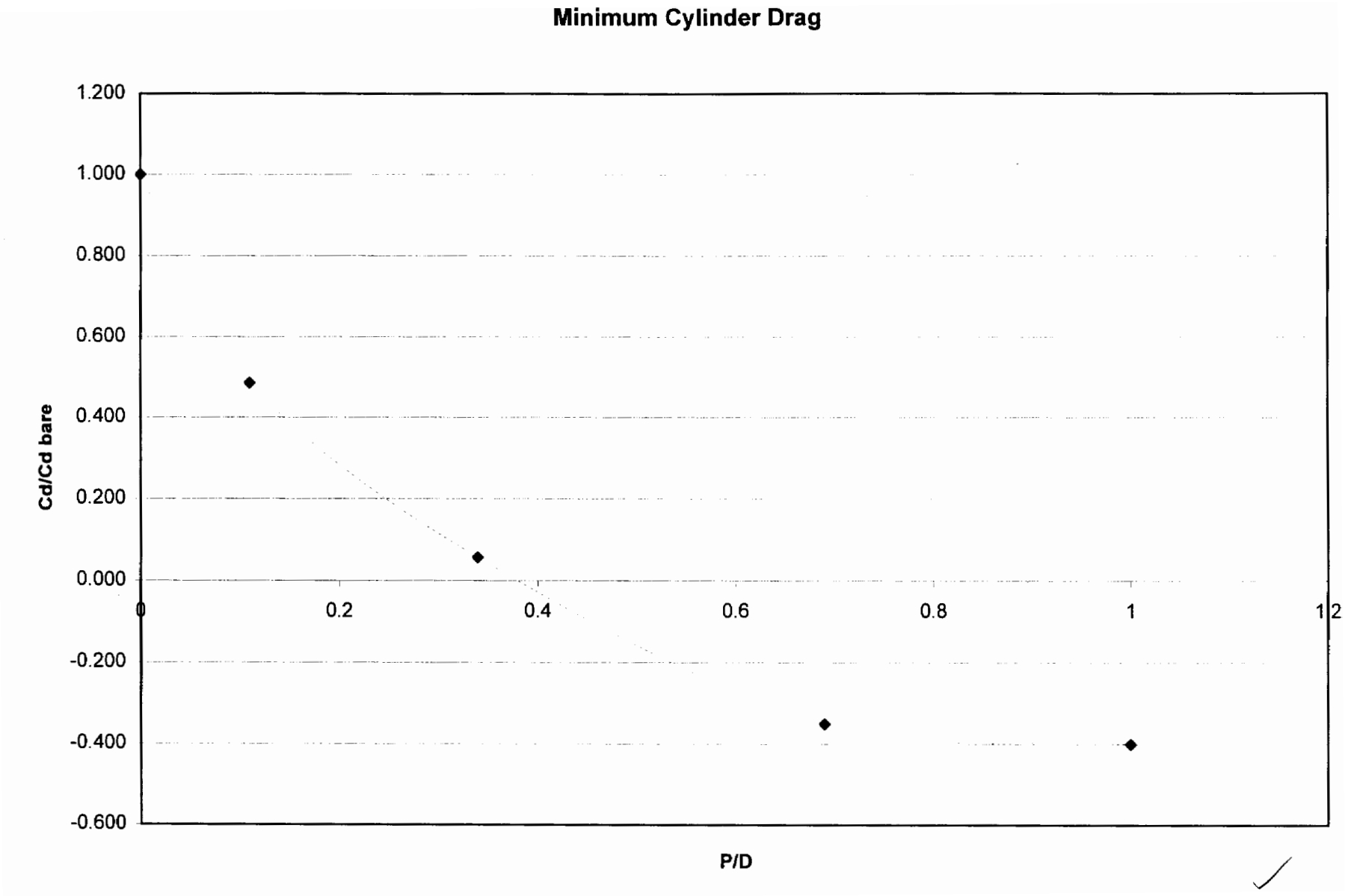
Minimum Cylinder Drag
1.200
1.000
0.800
0.600
0.400
0.200
0.000
-0.200
-0.400
-0.600
Cd/Cd bare
0
0.2
0.4
0.6
0.8
1
1.2
P/D

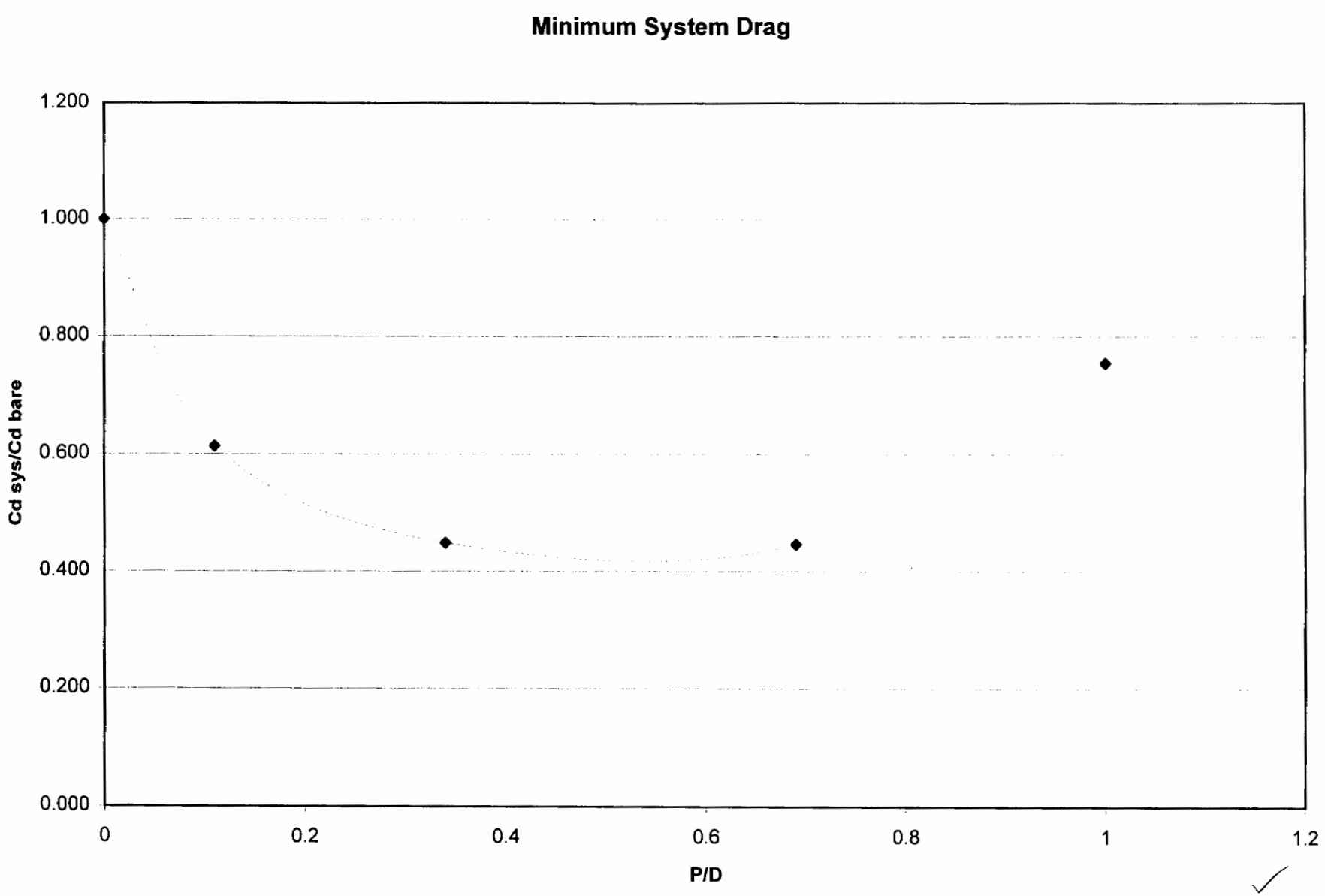

✓

- It is good to label the optimum point/regio